Taylor & Francis
Taylor & Francis Group

Computer Methods in Biomechanics and Biomedical Engineering

ISSN: 1025-5842 (Print) 1476-8259 (Online) Journal homepage: https://www.tandfonline.com/loi/gcmb20

A mathematical musculoskeletal shoulder model for proactive ergonomic analysis

Clark R. Dickerson , Don B. Chaffin & Richard E. Hughes

To cite this article: Clark R. Dickerson , Don B. Chaffin & Richard E. Hughes (2007) A mathematical musculoskeletal shoulder model for proactive ergonomic analysis, Computer Methods in Biomechanics and Biomedical Engineering, 10:6, 389-400, DOI: 10.1080/10255840701592727

To link to this article: https://doi.org/10.1080/10255840701592727

Published online: 29 Oct 2007.

Submit your article to this journal

Article views: 1222

View related articles

Citing articles: 12 View citing articles

Full Terms & Conditions of access and use can be found at
https://www.tandfonline.com/action/journalInformation?journalCode=gcmb20

Computer Methods in Biomechanics and Biomedical Engineering,
Vol. 10, No. 6, December 2007, 389–400

Taylor & Francis
Taylor & Francis Group

A mathematical musculoskeletal shoulder model for proactive ergonomic analysis

CLARK R. DICKERSON†*, DON B. CHAFFIN‡¶ and RICHARD E. HUGHES‡§

†Department of Kinesiology, University of Waterloo, Waterloo, Canada
‡Department of Biomedical Engineering, University of Michigan, Ann Arbor, USA
¶Center for Ergonomics, University of Michigan, Ann Arbor, USA
§Department of Orthopaedic Surgery, University of Michigan, Ann Arbor, USA

(Received 19 December 2005; in final form 19 March 2007)

Occupational shoulder musculoskeletal injuries and disorders are common. Generally available shoulder work analysis tools do not offer insight into specific muscle load magnitudes that may indicate increased risk, nor do they address many concerns germane to job analysis. To address these issues, a biomechanical model of the shoulder was developed to include several critical components: the systematic inclusion of kinematic and kinetic effects, population scalability, geometric realism, an empirical glenohumeral constraint, and integration with digital ergonomics analysis software tools. This unique combination of features in a single model was explored through examination of both experimental and simulated data with the developed analysis tool. The utility of the model is discussed together with a review of its specific strengths and weaknesses, and the potential for its future use in proactive ergonomic analyses and workplace simulations.

Keywords: Proactive ergonomics; Biomechanics; Optimization; Shoulder; Musculoskeletal model

1. Introduction

Practicing ergonomists and safety professionals need better analysis tools for the evaluation of occupational shoulder muscular demand. *A priori* knowledge of specific occupational muscle force and stress levels would help to enable the proactive prevention of shoulder disorders (Herberts *et al.* 1984). Current field and job design analysis tools are insufficient for this purpose, as they rely on indirect load estimates obtained by limited observation of existing jobs (McAtamney and Corlett 1993, Moore and Garg 1995, Latko *et al.* 1997). In addition, ergonomics software exists for the calculation of externally generated static joint moments and loads (Chaffin 1997), for both actual and virtual situations, but calculates neither tissue nor joint loadings.

Conversely, although a significant amount of progress has been made towards estimating shoulder tissue loads, developed models are not well integrated into ergonomic analyses. This progress has taken the form of several high-fidelity computerized and theoretical shoulder musculoskeletal models and their derivatives (Hogfors *et al.* 1987, 1991, 1995, Dul 1988, Wood *et al.* 1989a,b, Veeger *et al.* 1991, Karlsson and Peterson 1992, Van der Helm 1994a,b, Nieminen *et al.* 1995, Niemi *et al.* 1996, Hughes and An 1997, Soechting and Flanders 1997, Laursen *et al.* 1998, 2003, Garner and Pandy 1999, 2000, 2001, 2003, Makhsous 1999, Charlton and Johnson 2001, Holzbaur *et al.* 2005). While these existing shoulder models incorporate many biomechanical concepts central to shoulder function, they were not developed for prospective ergonomic field use. This resulted in the concomitant unavailability of several features within currently available models: (1) intersegmental dynamics, (2) population scalability, (3) rapid online depiction of realistic geometry, (4) an empirical shoulder stability constraint, (5) integration with commercial ergonomics software, including digital human modeling (DHM) and task analysis packages. Many models are either strictly static (Hogfors *et al.* 1987, 1991, 1995, Dul 1988, Karlsson and Peterson 1992, Niemi *et al.* 1996, Hughes and An 1997, Laursen *et al.* 1998, 2003, Makhsous 1999, Holzbaur *et al.* 2005) or do not fully explain their dynamic capability (Wood *et al.* 1989a,b, Hogfors *et al.* 1995, Charlton and Johnson 2001, Garner and Pandy 2001, 1999, 2000, 2003). Several other models are not

*Corresponding author. Email: cdickers@uwaterloo.ca

Computer Methods in Biomechanics and Biomedical Engineering
ISSN 1025-5842 print/ISSN 1476-8259 online © 2007 Taylor & Francis
http://www.tandf.co.uk/journals
DOI: 10.1080/10255840701592727

population scalable (Wood *et al.* 1989a,b, Veeger *et al.* 1991, Van der Helm 1994a,b, Soechting and Flanders 1997, Laursen *et al.* 1998, 2003, Garner and Pandy 1999, 2000, 2001, 2003). Online realistic musculoskeletal visualization is missing from other models as well (Dul 1988, Wood *et al.* 1989a,b, Karlsson and Peterson 1992, Nieminen *et al.* 1995, Niemi *et al.* 1996, Hughes and An 1997, Soechting and Flanders 1997, Laursen *et al.* 1998, 2003, Makhsous 1999). The empirical stability constraint is unique to this model. Similarly, no other model is designed to interface with available ergonomics software, particularly those that depend on experimental electromyography measurements (Soechting and Flanders 1997, Laursen *et al.* 1998, 2003). This model integrates these features into a single, accessible model. Doing so creates the novel and highly desirable capacity to perform rapid, proactive job analyses.

The objectives of this paper are to describe and demonstrate the computational shoulder musculoskeletal model designed to contain and exploit these desirable features.

2. Materials and methods

2.1 The overall shoulder model

The shoulder model is a composite of three linked modules (figure 1): (1) a musculoskeletal geometry module; (2) an external dynamic joint moment module; and (3) an internal muscle force prediction module. The inputs for each module derive from three sources: subject data; motion data; and task data, and can be either simulated or empirically gathered. While the geometric and moment modules are entirely independent of one another, their combined outputs serve as the primary inputs to the force prediction module. All of the modules were built in the Matlab® software package. The intentional modular design will facilitate future model modifications, as improved geometric and morphological data becomes available. The model is currently a unilateral, right-sided model.

2.2 The shoulder geometry module

The geometric module has five parts: (1) segment parameter definition; (2) shoulder rhythm implementation; (3) muscle definition; (4) muscle line-of-action construction; and (5) other geometric definitions. The geometric model uses 3D postural motion files as input. These files contain the Cartesian coordinates of body landmarks during a motion, defined in a global reference system. The reference system has the positive x-axis directed laterally to the right, the positive y-axis directed forward, and the positive z-axis directed up. The model outputs the positions and orientations of the defined segments, and the lines-of-action (L-O-A) and accompanying functional moment arms of each defined muscle element.

2.2.1 Segment parameter definitions. There are five segments defined in the model, which are consistent with an existing model (Hogfors *et al.* 1987, 1991, 1995, Karlsson and Peterson 1992, Makhsous 1999): the scapula, the clavicle, the humerus, the torso, and a combined radial/ulnar forearm link. The sternoclavicular, acromioclavicular, and glenohumeral joints are modeled as spherical joints with three degrees of rotational freedom, but no translational degrees of freedom. The elbow joint is modeled as having one degree of freedom (anatomical flexion/extension). The length of the thoracic torso is defined as 70% of the distance between the midpoint of the first thoracic and fifth lumbar vertebrae. Segment lengths are calculated based on torso length with published proportions (Makhsous 1999). The coordinate systems described by Hogfors *et al.* (1987) require access to or estimates of internal bony landmarks that are inaccessible *in vivo*. To analyse data collected from living subjects, the spatial location of these bony landmarks are estimated in the model by techniques described by

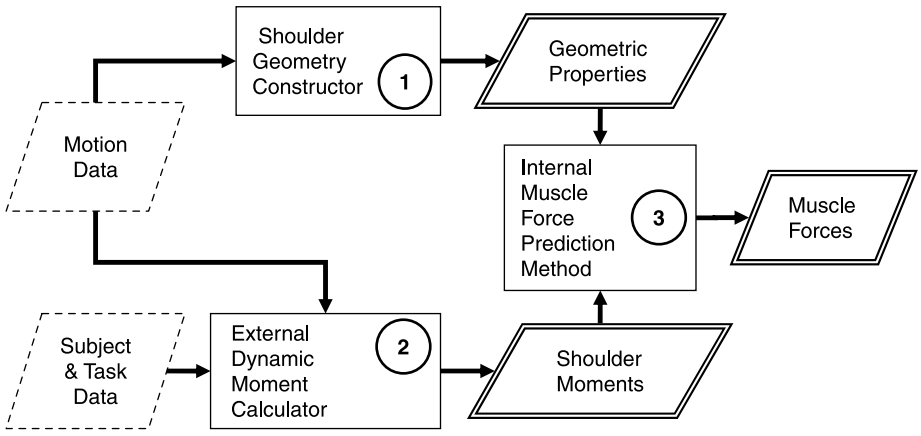

Figure 1. Data flow through the mathematical shoulder model. The model inputs are motion, subject and task data. Inputs are framed with dashed lines and outputs with double lines. Model segments are numbered and indicated by single-lined boxes.

Nussbaum and Zhang (2000), allowing replication of the segmental coordinate systems. The definitions of these coordinate systems, as well as the Euler convention used are described in section 2.4 in the description of the external module.

2.2.2 A modified shoulder rhythm algorithm. A humeral–thoracic shoulder rhythm that is consistent with our segmental coordinate systems has been reported (Makhsous 1999), which was extrapolated from previously studied rhythms (Hogfors *et al.* 1991, Karlsson and Peterson 1992). This rhythm is mathematically modified in the model to allow the model to accommodate experimentally collected data. The basis for the modification is the difference between landmarks used between a previous model (Hogfors *et al.* 1987) and the current model. Following application of the above shoulder rhythm, the scapula is further constrained to maintain its inferior and superior angles in narrow ranges outside the ribcage, which is defined by a 3D cylindrical surface. These positions are found through sequential single-degree modification of the scapular Euler angles until a position satisfying this constraint is found.

2.2.3 Muscle definitions. There are 23 muscles in the model. However, several muscles are modeled as multiple mechanical elements: latissimus dorsi (2 elements), serratus anterior (3), trapezius (4), subscapularis (3), infraspinatus (2), pectoralis major (2), deltoid (3), biceps (2), and the triceps (3), resulting in 38 muscle elements. Published segment-specific muscle attachment site average locations for our model coordinate systems are used to place muscle elements (Dul 1988). These are expressed as fractional distances along each segment local axis, in proportion to segment length. These data are combined with 3D orthopaedic geometric representations derived from the visible human dataset to confirm and finalize the muscle attachment sites on each bone.

2.2.4 Muscle line-of-actions. Muscle L-O-As are generally modeled as strings connecting defined muscle attachment sites. However, this convention generates improper L-O-As for several muscles (Van der Helm 1994b). In these cases, the L-O-As are modified to pass around orthopaedic barriers, specifically the ribcage and humeral head. To achieve these muscle paths, variations of spherical and cylindrical (Van der Helm 1994b, Charlton and Johnson 2001) geometric muscle wrapping techniques are used. Muscles wrapped using the spherical technique are three rotator cuff muscles (supraspinatus, infraspinatus, and subscapularis) and the deltoid. The cylindrical technique is used to wrap the serratus anterior. Before wrapping a L-O-A, a wrapping type-specific collision detection procedure assesses the need to wrap each specific muscle in the current posture. This prevents the unnecessary alteration of muscle moment arms in many cases, while ensuring it in others.

2.2.5 Other geometric parameters. Additionally, two scapulothoracic contact force application sites (Makhsous 1999) located at the inferior and superior angles of the scapula are specified to reflect forces transmitted to the scapula from contact with the posterior ribcage. Ligaments are also placed according to literature data (Hogfors *et al.* 1987, Makhsous 1999), but are not functional in the current model as muscles have been shown to be the primary generators for producing joint moments (Crowninshield and Brand 1981a,b, Jinha *et al.* 2006).

2.3 The external dynamic shoulder moment model

The shoulder moment model is partially adapted from an existing inverse dynamics methodology used to study human gait kinetics (Vaughan *et al.* 1992). This model has four parts: (1) segment property description; (2) linear kinematics; (3) angular kinematics; and (4) computation of joint forces and moments. Model inputs are motion files and time-series external force profiles. Model outputs are continuous dynamic joint moment and force values caused by external forces for a task. Computational details of this model were previously detailed (Dickerson *et al.* 2006), but are also summarized here

2.3.1 Segment property description. The right arm is modeled as a three-segment linkage composed of the upper arm, forearm and hand. Individual segment mass values and directional moments of inertia are calculated using anthropometric data (stature and body weight) as inputs to the reported regression prediction equations (Zatsiorsky and Seluyanov 1993).

Motion data is used to calculate relevant joint center locations using methods developed for a reduced marker set (Nussbaum and Zhang 2000). The joint centers estimated are the glenohumeral (represented by the center of the humeral head), the elbow, and the wrist joints. From these joint centre locations, the spatial locations of the centers of mass (CMs) of each segment are calculated based upon reported CMs/segment-length ratios (Clauser *et al.* 1969).

2.3.2 Linear kinematics. Velocity and acceleration of the segment centers of gravity are determined using numerical differentiation. The first and second derivatives of the displacement–time data are calculated using standard difference equations:

$$\frac{\partial x_n}{\partial t} = \dot{x}_n = \frac{x_{n+1} - x_{n-1}}{2\Delta t} \tag{1}$$

and

$$\frac{\partial^2 x_n}{\partial^2 t} = \ddot{x}_n = \frac{x_{n+1} - 2x_n + x_{n-1}}{(\Delta t)^2} \tag{2}$$

where x, a data point; n, the nth (current) frame and Δt is the time between consecutive frames. Prior to performing numerical differentiation, experimentally-derived data are filtered using a Matlab® second-order Butterworth low-pass filter set to a cut off frequency of 6 Hz. The suitability of this cut off has been verified through frequency analysis of a large experimental data set, to confirm that the power of the signal was negligible beyond half of the selected frequency, or 3 Hz.

The neutral arm posture is defined as having the arm extended to the side, perpendicular to the torso, with palms down. Local coordinate systems were defined for each segment according to the definitions of Hogfors *et al.* (1987).

2.3.3 Angular kinematics. A derivative of an Euler angle based technique known as the joint coordinate system (JCS) technique (Nigg and Herzog 1994) is applied to assess segmental rotations. The first rotation is about the flexion/extension axis of the joint (ψ, the second rotation is about the abduction/adduction axis (θ), and the third rotation is about the longitudinal segment axis (ϕ). These are slightly different permutations for the three different arm segments. Two rotations are used to describe segmental angle configurations. The first, a 3-2-1 transformation is used to describe the orientations of the upper arm and forearm:

$$\begin{Bmatrix} x \\ y \\ z \end{Bmatrix} = \begin{bmatrix} \cos\psi\cos\theta & \sin\psi\cos\theta & -\sin\theta \\ (-\sin\psi\cos\phi + \cos\psi\sin\theta\sin\phi) & (\cos\psi\cos\phi + \sin\psi\sin\theta\sin\phi) & \cos\theta\sin\phi \\ (\sin\psi\sin\phi + \cos\psi\sin\theta\cos\phi) & (-\cos\psi\sin\phi + \sin\psi\sin\theta\cos\phi) & \cos\theta\cos\phi \end{bmatrix} \begin{Bmatrix} X \\ Y \\ Z \end{Bmatrix} \tag{3}$$

The orientation of the hand, due to its different neutral orientation, is described by a 2-3-1 transformation matrix:

$$\begin{Bmatrix} x \\ y \\ z \end{Bmatrix} = \begin{bmatrix} \cos\psi\cos\theta & \sin\theta & -\sin\psi\cos\theta \\ (\sin\psi\sin\phi - \cos\psi\sin\theta\cos\phi) & \cos\theta\cos\phi & (\cos\psi\sin\phi + \sin\psi\sin\theta\cos\phi) \\ (\sin\psi\cos\phi + \cos\psi\sin\theta\sin\phi) & -\cos\theta\sin\phi & (\cos\psi\cos\phi - \sin\psi\sin\theta\sin\phi) \end{bmatrix} \begin{Bmatrix} X \\ Y \\ Z \end{Bmatrix} \tag{4}$$

In both equations (3) and (4), X, Y, and Z are global 3D coordinates and x, y, and z are local 3D coordinates.

The segmental angular velocities and accelerations are determined through classical mechanical methods (Vaughan *et al.* 1992). These are functions of the Euler angles and their first and second derivatives. The time derivatives of the Euler angles are determined using the same finite differencing technique described for linear kinematics.

2.3.4 Calculation of joint forces and torques. In the force equilibrium calculation, derived from the linear form of Newton's second law of motion is applied for each segment using the following equilibrium for each segment:

$$\sum F = m_{\text{segment}} \times a_{\text{COM,segment}} \tag{5}$$

where F, forces; m, mass of segment and a, acceleration of segment COM. External forces in most cases are the hand forces and the weights of the segments. Solving the resulting equation achieves the external joint load at each proximal joint segment.

To calculate torque values, the angular analog of Newton's second law is applied to each segment:

$$\sum M = \dot{H} \tag{6}$$

where M, external torque and $\dot{H}$, rate of change of segmental angular momentum.

The rate of change of angular momentum is calculated based on the segmental moments of inertia and the segmental velocities and accelerations. External torques are calculated based on the cross products of the produced forces and their lever arms, using a variation of an existing method (Vaughan *et al.* 1992). Applying segmental equilibrium sequentially, the torques are calculated at the proximal ends of each segment.

2.4 Muscle force prediction model

The third, final model stage is the muscle force prediction module. The shoulder is an indeterminate mechanical system, due to the large number of muscle elements (38 in our model formulation) compared to the number of mechanical equilibrium conditions defined in the system (19 as described in 2.5.1). The prospective nature of the ultimate model application led to the choice of a numeric optimization approach to solving the load distribution problem amongst the muscles. Optimization techniques have been used extensively in the prediction of muscular

force in the shoulder (Hogfors *et al.* 1987, 1991, 1995, Dul 1988, Veeger *et al.* 1991, Van der Helm 1994b), as well as other joints (Crowninshield and Brand 1981a,b, Herzog and Binding 1993, Hughes *et al.* 1994). The muscle module has five parts that both delimit the solution space and ensure a unique solution: (1) mechanical equilibrium constraints; (2) muscle force bounds; (3) a glenohumeral joint force constraint; (4) a governing objective function; and (5) a solution methodology.

2.4.1 Mechanical equilibrium constraints. In the optimization solution, there are 19 mechanical equilibrium constraints. Six equilibrium equations address 3D angular and linear equilibrium of each of the defined segments about the glenohumeral, acromioclavicular, and sternoclavicular joints. The final equilibrium equation constraint is for the elbow flexion/extension moment. The form of these constraints is analogous to those of the external moment model, with several more force contributors, specifically the muscles. The general linear formulation of the force constraints is as follows:

$$\sum F_{\mathrm{m},i} + J_{i-1} + J_i = \sum F_{\mathrm{E}} \tag{7}$$

where $F_{\mathrm{m},i}$ are the muscles active on segment i, J_{i-1} is the joint contact force on the distal joint, J_i is the joint contact force on the proximal joint, and F_{E} are any external forces unaccounted for in the previous segmental calculations. This is of particular importance for the clavicle and scapula systems, which are considered to have zero mass and zero acceleration.

The angular general case is also similar to the formulation in the external model:

$$\sum (l_i \times F_{\mathrm{m},i}) + \tau_{i-1} + \tau_i = \sum \tau_{\mathrm{E}} \tag{8}$$

where l_i is the moment arm of the ith muscle, and the moment terms (τ's) are analogs of the force terms from the previous equation.

2.4.2 Muscle force bounds. Muscle forces act along L-O-As generated by the geometric shoulder model as defined by unit vectors. These forces are constrained to remain nonnegative, as they are not allowed to transmit force in tension. Thus the lower bound for all muscle tensile forces is zero. The maximum value of tensile force allowed in a muscle, u_i, is assumed to be in proportion to the physiological cross-sectional area (PCSA) of the specific muscle. The baseline value for in the model is estimated to be a specific tension of $88\,\mathrm{N\,cm^{-2}}$ (Wood *et al.* 1989a). The values for individual muscle PCSA were obtained from the published results of a cadaver study (Hogfors *et al.* 1987).

2.4.3 Glenohumeral contact force constraint. Our model uses empirical cadaver data on directional glenohumeral joint dislocation force ratios (Lippitt and Matsen 1993) to form three additional constraints. These data were converted into a set of linear equations that describe the glenohumeral contact force dislocation ratio thresholds along eight equally spaced compass directions, which are perpendicular to the glenoid surface. The dislocation force is calculated as part of the optimization solution in a global coordinate system. The directional dislocation ratio thresholds, originally calculated in the local (glenoid) system, are converted into the global system using a local-to-global transformation matrix. The components in each global system axis are combined into an equation (yielding one in each global direction). The glenohumeral contact force was also required to not exceed any directional dislocation ratio threshold, thus maintaining a theoretically non-dislocating glenohumeral joint. Further, the glenohumeral contact force was required to be a linear, nonnegative combination of values in each global direction that did not exceed the stability requirement. The constraints are of the general form (repeated for each global direction):

$$J_{\mathrm{gh}} = \sum_{i=1}^{8} c_i S_i \quad \text{given that :} \quad c_i \geq 0 \tag{9}$$

where J_{gh}, glenohumeral joint contact force; c_i, the ratio coefficient in the ith glenoid orientation and S_i; glenohumeral joint dislocation force ratio thresholds in the ith glenoid orientation. The values used for the directional force ratio thresholds are found in figure 2. They are calculated as follows from the data of Lippitt and Matsen (1993):

$$S_i = \frac{F_{\mathrm{s},i}}{F_{\mathrm{c}}} \tag{10}$$

where $F_{\mathrm{s},i}$ is the shear force in the ith direction, and F_{c} is the compressive force directed perpendicularly into the glenoid cavity.

2.4.4 Optimization objective function. The objective function Θ is defined as (Nieminen *et al.* 1995, Laursen *et al.* 1998):

$$\Theta = \sum_{i=1}^{38} \left(\frac{f_i}{\mathrm{PCSA}_i} \right)^3 \tag{11}$$

where f_i is the force prediction for muscle i, and PCSA_i is the cross-sectional area (CSA) of muscle i. This cost function provides similar results to cost functions previously suggested for shoulder models (Dul 1988, Chaffin 1997). This function is promotes synergistic muscle load sharing amongst agonistics for a range of loading scenarios, compared to other models (Herzog and Binding 1993).

2.4.5 Solution methodology. The indeterminacy of the mechanical system modelled is solved sequentially at each

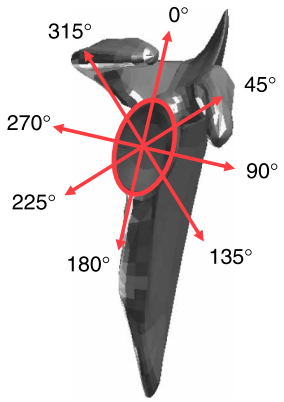

Direction	Dislocation Force Ratio Threshold (Shear/Compression) (%)
0	51
45	33
90	29
135	40
180	56
225	43
270	30
315	35

Figure 2. Directional shoulder dislocation force threshold ratios. Ratios indicate the directional shear to compressive force joint dislocation tolerance. Note that the glenoid fossa is not a perfect ellipse, but is directionally asymmetric. This asymmetry is incorporated into the constraints detailed in section 2.5.3.

interval of the motion file, and this solution is used by the subsequent iteration as the initial condition for the optimization. The optimization scheme has a standard form:

$$\text{Minimize } \Theta \tag{12}$$

$$\text{s.t. } \mathbf{Ax} = \mathbf{B} \quad \text{(linear equality constraints)} \tag{13}$$

$$0 \le f_i \le u_i \quad \text{for } i = 1, \ldots, 38 \quad \text{(muscle force bounds)} \tag{14}$$

In our model, there are 22 equality constraints, 19 derived from mechanical equilibrium and three related to the glenohumeral contact force. Solving for 60 unknown variables results in the formation of a 22 × 60 matrix (**A** in equation (13)) and a 22 × 1 matrix (**B** in equation (13)).

In addition, the muscle force bounds (from zero to u_i) are implemented as boundary constraints (equation (14)). The unknown variables solved for by the model (**x** in equation (13)) are muscle forces levels (38), ligament forces (3), joint contact forces (9), scapulothoracic contact forces (2), and directional dislocation force ratio coefficients (8), for a total of 60 scalar quantities. These solutions form a 60 × 1 matrix (**x** in equation 13) for each model evaluation. Ligament forces are not currently active in the model, but they may be activated in future analyses if appropriate.

2.5 Model evaluation

There are three types of model outputs: geometric, joint kinetics, and tissue loading. These provide insight into aspects of the mechanical response of the body to task performance. Simulated and experimental tasks were used to highlight the ability to address important ergonomic queries.

2.5.1 Simulated tasks. The task simulated to exercise the shoulder model was a load holding task. Geometric postural data was obtained with the 3DSSPP program, which is the most popular computer software used in ergonomic analysis (Dempsey *et al.* 2005). The location of the hand was set in the program as (+23.5 cm horizontal (forward), + 110 cm vertical (upward), + 20 cm lateral (right)). The (0, 0, 0) point, or origin, in 3DSSPP is located between the bases of the feet. Maintaining identical positioning of right hand in space, the anthropometry of the subject was varied to be equal to that of a 5th-percentile female, a 50th-percentile female, a 50th-percentile male, and a 95th-percentile male, using the built-in posture prediction algorithms of the program. This resulted in different postures for each simulated anthropometry. For each anthropometry, the hand load was varied from 0 to 100 N in 20 N increments. External shoulder joint moments, muscle force estimates, and internal joint contact forces (including muscular activations) were calculated by using the shoulder model to analyze the 3DSSPP posture/load combinations.

2.5.2 Use of empirical data to display model functionality. In addition, experimental trials were processed using the biomechanical model. The trials used to demonstrate the model consisted of dynamic loaded reaches in the sagittal plane, which were held for 3 s before the reach was reversed. The load in the hand was varied in these reaches between 0, 25, and 50% of extended arm shoulder flexion strength. Kinematics, anthropometrics, and task exposures were recorded as inputs to the model.

2.5.3 Comparison to an existing shoulder musculoskeletal model. To compare the outputs of the model with an existing model (Van der Helm 1994b), muscle activations were predicted for unloaded arm abduction at 10° increments from −90 to 60° abduction

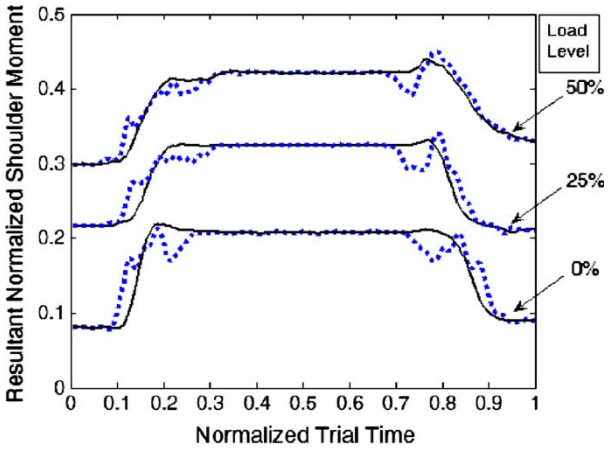

Figure 3. The impact of dynamic terms on moment calculations for three hand force levels (0, 25, and 50% of shoulder elevation strength). Dynamic calculations are shown with dotted lines, and static calculations with solid lines. Although the instantaneous values vary during the movement phases of the reaches, the overall (integrated) amount of moment at the shoulder remains constant for the analyses.

as defined relative to the neutral posture. The anthropometry used was a male with a height of 1.78 m and a body mass of 80 kg. The compared model (Van der Helm 1994b) states that their model is based upon "a more or less median cadaver". Graphical comparisons were made with available data. This simulation also highlights the capability of executing the computational model using Euler-angle based posture definitions.

2.5.4 Variation of the glenohumeral joint contact force constraint. Variation of the constraint caused changes in model muscle force predictions. These were primarily changes in the level to which specific muscles were activated for a given load/posture combination. To demonstrate this, a stability multiplier, ϑ, was varied from 0.4 to 1.0 by increments of 0.2. This multiplier was then applied to the dislocation force ratio thresholds. A multiplier value of 1.0 represents allowing shear forces equal to the magnitude of the directional dislocation force ratio thresholds.

3. Results

The model incorporates several aspects previously unavailable concurrently in existing job analysis tools. These include the impact of dynamics on shoulder loads, stature scalability, rapid online geometric realism, an empirical glenohumeral contact force constraint, and integration with widely-used current ergonomics software packages. Previously, outputs such as predicted specific muscle activations and joint contact forces were unavailable for many ergonomists.

3.1 The impact of dynamics

The inclusion of kinematics and kinetics in the calculation of joint moments reveals that information is lost in a strictly static analysis of collected empirical data (figure 3). This is prominent during the launch and return phases of the experimental loaded reaches. The impact of dynamics, as a percentage, is higher in reaches with lower masses, as segmental kinetic contributions represented a larger portion of the overall shoulder exposure. The impact of dynamics is minimal during the hold phase, as no motion effects are present and the moments values become purely hand load and segment weight generated.

3.2 Anthropometric variation

A second important aspect of the model is its ability to perform operations on a range of different anthropometries through global model scaling, as this is a highly desirable capability in ergonomic design. The simulations performed for the seated reach tasks show the range of values obtained with the model for both shoulder moments and glenohumeral contact forces (figure 4). These values

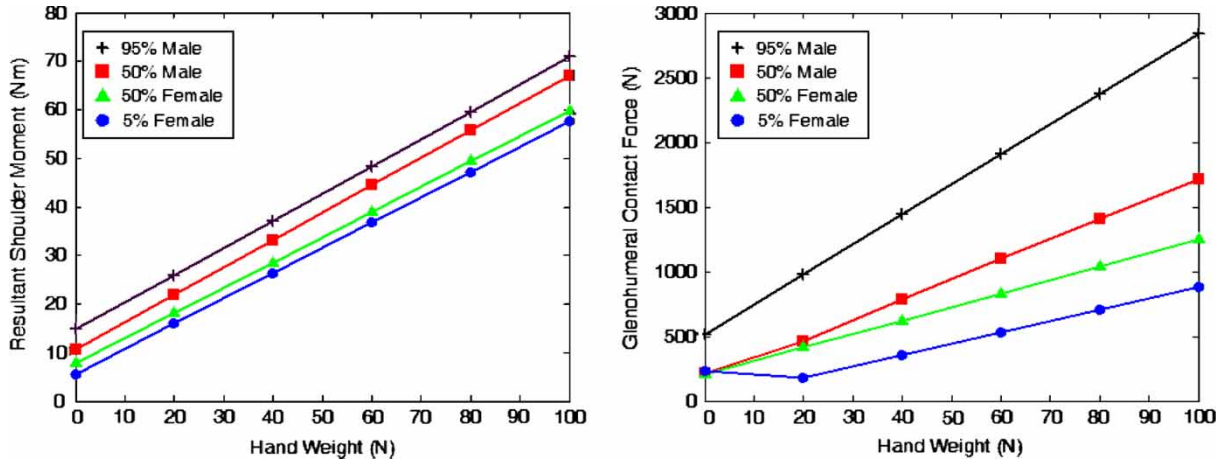

Figure 4. Shoulder moments and glenohumeral contact forces for four different anthropometries during a load holding task: 95% male, 50% male, 50% female, and 5% female. These values incorporate body mass and anthropometry, along with posture prediction through ergonomic software algorithms.

are an integration of the subject weight, dimensions, and the externally applied forces. Note that there is never a zero moment or contact force level as the weight of the arm is omnipresent.

3.3 A geometrically realistic mathematical shoulder representation

An important aspect of our model is the ability to render a detailed geometric representation of the musculoskeletal system in a range of postures. The geometric depiction includes bones scaled to the subject anthropometry as well as visual representations of all of the muscle L-O-A (figure 5). This allows quick investigation and understanding of the capabilities of each muscle element in various postures, facilitating interpretation of the model outputs and posture-dependent variations in model predictions.

3.4 Influence of the glenohumeral contact force constraint

A more restrictive dislocation force ratio requirement (indicated by a lower value of the stability multiplier) resulted in increased values for muscular load predictions (figure 6). This was somewhat different in dissimilar postures. Muscle switching also occurred depending on the level of stability control, and varied across postures.

3.5 Integration with ergonomic analysis software

Postural data can be shared from ergonomics software such as Jack or 3DSSPP. This was demonstrated by importing posture data from 3DSSPP to provide postures as inputs to the model. Similarly, postures from Jack can currently be reconstructed using the model. One primary goal is the seamless integration of the model with computerized tools to enable proactive design analysis capability.

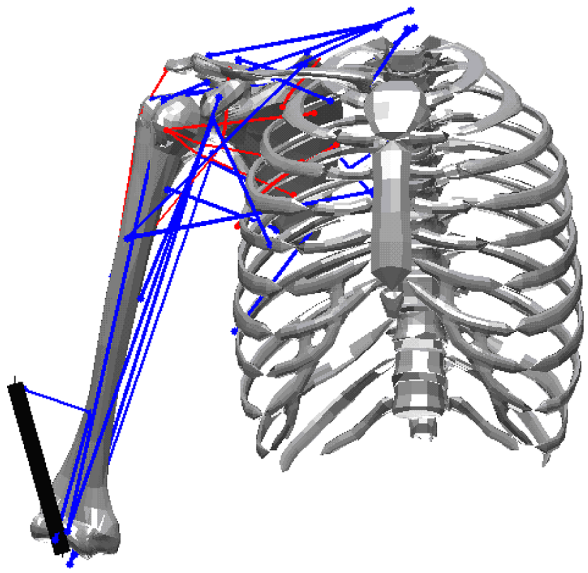

Figure 5. Depiction of glenohumeral internal geometry, including bones and muscle elements.

3.6 Comparison of model predictions with an existing computational model

Our computational model predicted activity in shoulder muscles that was similar to that predicted by a previous biomechanical model (Van der Helm 1994a,b). While differences exist (specific examples are shown in figure 7), the primary agonists display similar properties, especially the middle deltoid and upper trapezius. Similarly, many muscles are predicted inactive by both models, including the posterior deltoid and the sternal insertion of pectoralis major. Observed differences in other muscles are thought to be largely a function of different muscle element definitions, as well as a different value of specific tension used (88 vs 37 $\mathrm{N\,cm^{-2}}$), which brought several of the predictions of the comparison model (Van der Helm 1994a,b) closer to maximum activations.

4. Discussion

4.1 The utility of the biomechanical shoulder model

Our model represents an important step forward towards the integration of tissue biomechanics with ergonomic analysis in the shoulder. Though notable shoulder models precede ours (Hogfors *et al.* 1987, 1991, 1995, Dul 1988, Wood *et al.* 1989a,b, Veeger *et al.* 1991, Karlsson and Peterson 1992, Van der Helm 1994a,b, Nieminen *et al.* 1995, Niemi *et al.* 1996, Hughes and An 1997, Soechting and Flanders 1997, Laursen *et al.* 1998, 2003, Garner and Pandy 1999, 2000, 2001, 2003, Makhsous 1999, Charlton and Johnson 2001, Holzbaur *et al.* 2005), they are not in heavy use by practicing ergonomists (Dempsey *et al.* 2005). Our model allows flexibility in implementation along with an ability to execute the model on a common software platform, Matlab®. In addition to these practicalities, our model also incorporates variations on approaches to address the shoulder rhythm (Makhsous 1999) and glenohumeral stability (Lippitt and Matsen 1993). The major functional contribution of our model is the production of a flexible ergonomic analysis and design tool for the study of shoulder loading for a range of exertions that has a unique combination of capabilities.

4.2 Strengths of the shoulder model

The strengths of our newly formulated model are in two major groups: (1) benefits to ergonomic analysis and (2) increased physiological realism.

4.2.1 Improvements to ergonomic analysis. It is important in designing an ergonomic tool to ensure that it can be applied to a diverse population, rather than for a

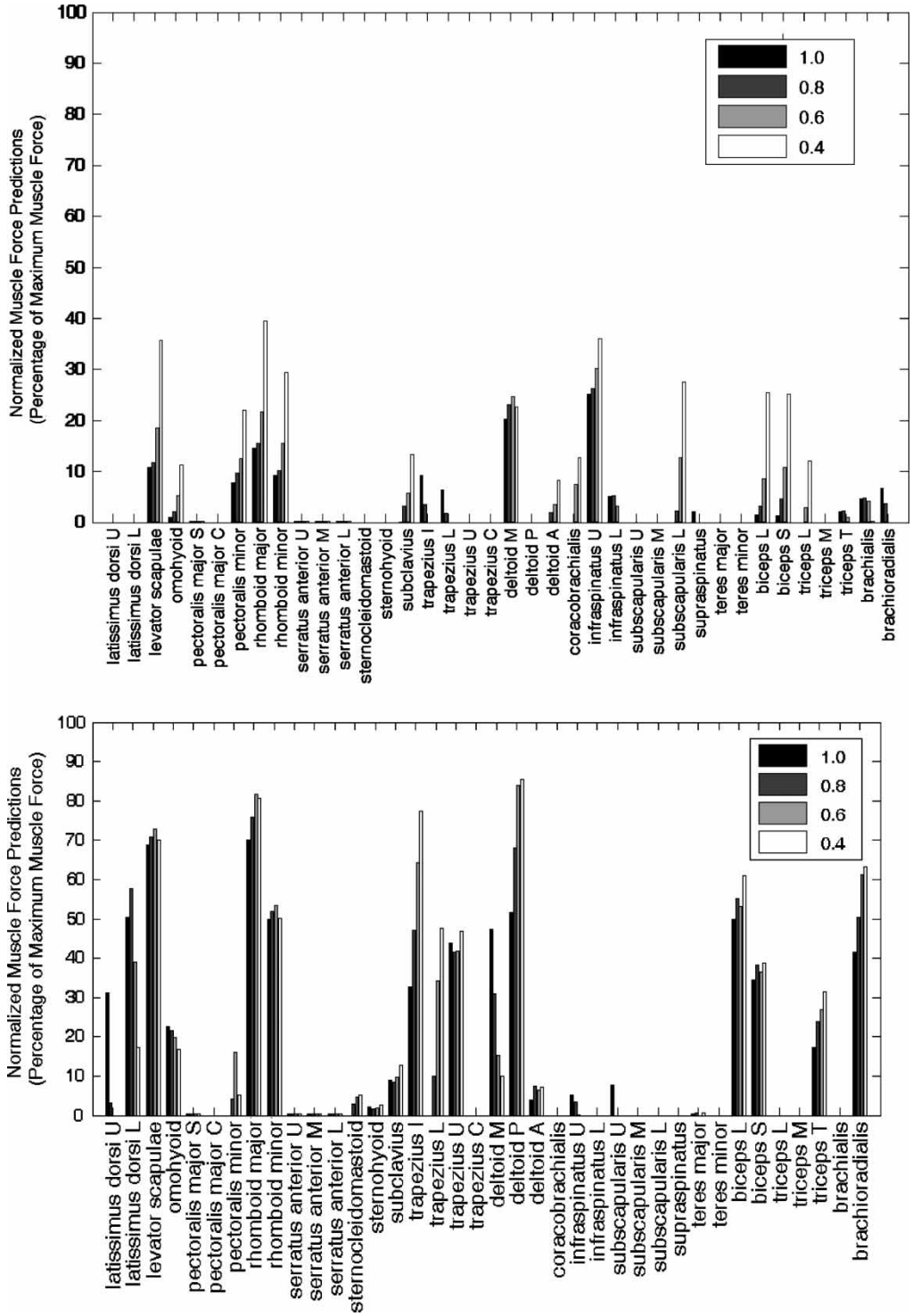

Figure 6. Effect of varying the stability multiplier, on muscle force predictions. ϑ was varied from 0.40 to 1.00 for two loading scenarios: (A) a forward reach along the 0° azimuth; (B) a diagonal (midway between sagittal and frontal planes) reach forward. Variation in both the active muscles and their magnitude of force production is evident, but more pronounced for the forward reach. Muscle names are indicated along the *x*-axis. Abbreviations: U, upper; L, lower and long (biceps and triceps); S, sternal and short (biceps); C, clavicular; M, middle and medial (triceps); I, intermediate and T, lateral.

specific group of individuals, such as clinical research may target. Our model addresses this through two scalability levels. The first is overall scalability of shoulder geometry. Bone lengths and muscle attachment sites scale relative to stature. This allows simulation of specific task requirements for an anthropometric spectrum (i.e. it can be used to estimate the difference in middle deltoid activity between a 2.0 m tall male and a 1.5 m female when lifting a 5 kg object from a parts bin to a work table). The model, if strength is known, can also be proportionately scaled to different maximum muscle capabilities, rather than using a default average value, as it currently does. Such flexibility addresses documented variations in population shoulder strength (Kumar 1991, Shephard 1995).

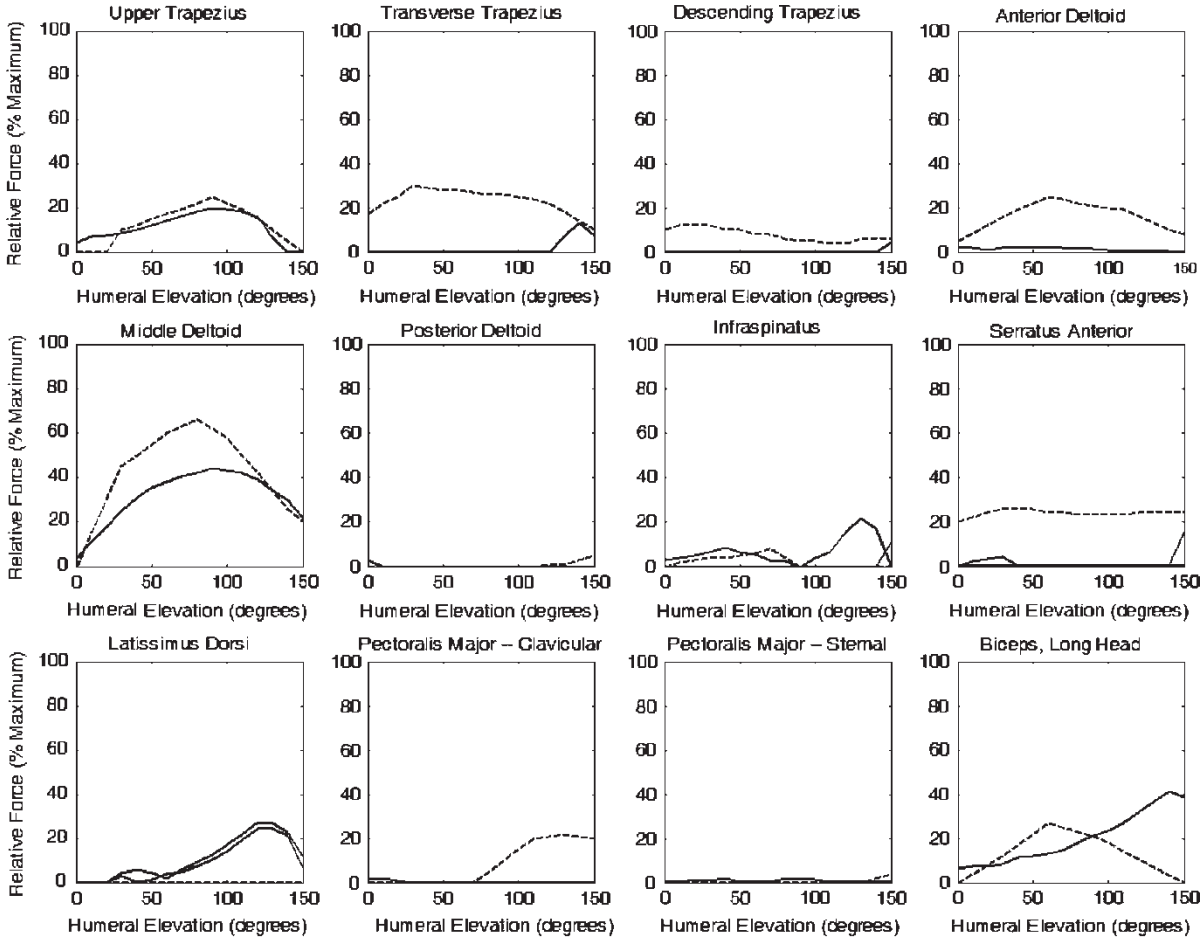

Figure 7. Muscle force prediction patterns for unloaded humeral abduction, as shown by our model (solid line) and an existing musculoskeletal model (dashed line). Muscles are indicated on the individual subplots. Muscles displayed were chosen on the basis of percentage of maximum values reported for an existing model (Van der Helm 1994a,b). The model also predicts forces in 26 additional muscles.

Many industrial tasks have a dynamic component to them. An advantage our biomechanical model has is the inclusion of dynamic terms in the estimation of the shoulder joint moments. These dynamic contributions also influence the muscle force prediction estimates, which are based directly upon the moments calculated. These steps toward a fully dynamic ergonomic analysis model are critical in replicating a large subset of industrial tasks.

A final contribution of the model to ergonomic analysis is the generation of a realistic geometric model of the human shoulder. The graphical representation of previous models is indistinct (Makhsous 1999), and for novice users is difficult to interpret. Inclusion of photorealistic orthopaedic structures allows the user to envision the potential contributions of the shoulder musculature in a given posture, as well as a means to understand the complex interplay between the bones in the shoulder girdle during a motion. This level of clarity is unprecedented in available model packages.

4.2.2 Improved physiological representation. The first novel aspect is the inclusion of an anisotropic, empirically-derived glenohumeral stability index. This index is an improvement as it represents directional non-dislocation requirements of the glenohumeral interface quantitatively. Previous attempts to address the issue of glenohumeral stability in a mathematical optimization model have used an ellipsoid cone into which the glenohumeral contact force is constrained to be directed (Hogfors *et al.* 1987, 1991, 1995, Veeger *et al.* 1991, Van der Helm 1994b, Nieminen *et al.* 1995, Niemi *et al.* 1996). A linear formulation of the empirical asymmetric stability requirements respects the known anisotropic characteristics of the glenohumeral joint beyond the capability of an ellipsoidal approximation. The current formulation also is composed of three linear constraints, which ensures a global optimization solution.

A second important aspect of the model is collision detection when determining muscle wrapping requirements. This explicit description of a technique to determine if modification of the muscle line-of action to respond to orthopaedic obstructions is needed adds to the realism of the model. Though the modeling of muscles as strings has inherent limitations, the ability of the model to respond to variations in posture and impose wrapping at appropriate times enhances the model's consistency and may help to identify insufficiencies present in wrapping algorithms.

4.3 Limitations of the biomechanical model

Although our model has many favourable aspects, it also has some limitations. These limitations generally relate to two areas: (1) possible misrepresentation of physiological processes and (2) potential insufficiency in characterizing biological variability.

4.3.1 Representation of muscle physiology. Two key muscle mechanics concepts known as the length–tension and velocity–tension relationships are not considered in the model. In doing this, the model assumes the same amount of force-producing capability in a muscle regardless of its instantaneous length and contraction velocity. However, variations in the shape of the length–tension curve for shoulder muscles have been shown to cause minimal changes in model predictions in a simulated study (Nieminen *et al.* 1995), and are suggested to have minimal effect in the physiological joint range of motion in the general case (Herzog and Binding 1993).

Ligamentous and capsular contributions were excluded based on the type of exertions targeted for the model studied. Ligaments are generally thought to primarily provide stability at the extremes of glenohumeral motion (Terry *et al.* 1991, Lippitt and Matsen 1993), which are atypical of the tasks of interest. Further, active muscle contractions are recognized as the primary contributors to the production of joint moments (Jinha *et al.* 2006). Also, due to the absence of ligamentous forces in the objective function, these quantities could skew results towards a more incorrect muscle loading profile.

Stiffness may be a result of cocontraction of antagonistic muscles when performing a task that requires precision, such as reaching to a given target in space (Hogan *et al.* 1987). In the current model, there is no implementation of a stiffness constraint for the humerus. Stiffness constraints have been shown to affect the predictions of a similar optimization based shoulder model (Nieminen *et al.* 1995). However, the general effect was a modest unsystematic increase in force levels for several muscles.

4.3.2 Model scalability. Assumptions required to enable model scalability may have the effect of discounting the impact of biological variability on individual muscle use fluctuations. First, a common average shoulder rhythm (Hogfors *et al.* 1987, Makhsous 1999) was applied to all subjects. Although the shoulder rhythm has been shown to be consistent for an individual, interindividual differences exist (Hogfors *et al.* 1987). Thus, a common rhythm may not truly reflect the relative scapular and clavicular motion of a given individual. This, however, should not lead to systematic errors in model predictions (Hogfors *et al.* 1991).

Similar arguments exist regarding our assumption that the proportionality of the CSAs of the shoulder muscles is constant across a population. However, variations in the total CSA of the shoulder muscles have demonstrated a negligible effect on the results of an optimization model of the shoulder (Nieminen *et al.* 1995). Data regarding CSA ratios for a population are unavailable.

5. Summary

We have created a shoulder model that combines several elements that are desirable to ergonomic designers. The model contains concurrent functionalities unavailable in existing shoulder model formulations. The major contribution of the work is the production of an ergonomic design analysis tool that allows prospective job design, and is compatible with existing popular ergonomics software. This bridge is an important step towards the universal inclusion of shoulder-specific analyses in job design and task analysis, and a significant enabler of simulation-based ergonomic research.

References

D.B. Chaffin, "Development of computerized human static strength simulation model for job design", *Hum. Factors Ergon. Manufact.*, 7(4), pp. 305–322, 1997.

I.W. Charlton and G.R. Johnson, "Application of spherical and cylindrical wrapping algorithms in a musculoskeletal model of the upper limb", *J. Biomech.*, 34, pp. 1209–1216, 2001.

C.W. Clauser, J.T. McConville and J.W. Young, *Weight, Volume and Center of Mass of Segments of the Human Body*, AMRL-TR-69-70 Dayton, OH: Aerospace Medical Research Laboratories, 1969.

R.D. Crowninshield and R.A. Brand, "The prediction of forces in joint structures: distribution of intersegmental resultants", *Exerc. Sport Sci. Rev.*, 9, p. 159, 1981a.

R.D. Crowninshield and R.A. Brand, "A physiologically based criterion of muscle force prediction in locomotion", *J. Biomech.*, 14, pp. 793–801, 1981b.

P.G. Dempsey, R.W. McGorry and W.S. Maynard, "A survey of tools and methods used by certified professional ergonomists", *Appl. Ergon.*, 36, pp. 489–503, 2005.

C.R. Dickerson, B.J. Martin and D.B. Chaffin, "The relationship between shoulder torques and the perception of muscular effort in load transfer tasks", *Ergonomics*, 49, pp. 1036–1051, 2006.

J. Dul, "A biomechanical model to quantify shoulder load at the workplace", *Clin. Biomech.*, 3, pp. 124–128, 1988.

B.A. Garner and M.G. Pandy, "A kinematic model of the upper limb based on the Visible Human Project (VHP) image dataset", *Comput. Methods Biomech. Biomed. Eng.*, 2, pp. 107–124, 1999.

B.A. Garner and M.G. Pandy, "The obstacle-set method for representing muscle paths in musculoskeletal models", *Comput. Methods Biomech. Biomed. Eng.*, 3, pp. 1–30, 2000.

B.A. Garner and M.G. Pandy, "Musculoskeletal model of the upper limb based on the visible human male dataset", *Comput. Methods Biomech. Biomed. Eng.*, 4, pp. 93–126, 2001.

B.A. Garner and M.G. Pandy, "Estimation of musculotendon properties in the human upper limb", *Ann. Biomed. Eng.*, 31, pp. 207–220, 2003.

P. Herberts, R. Kadefors, C. Hogfors and G. Sigholm, "Shoulder pain and heavy manual labor", *Clin. Orthop.*, 191, pp. 161–178, 1984.

W. Herzog and P. Binding, "Cocontraction of pairs of antagonist muscles: analytical solution for planar static nonlinear optimization approaches", *Math. Biosci.*, 118, pp. 83–95, 1993.

N. Hogan, E. Bizzi, F.A. Mussa-Ivaldi and T. Flash, "Controlling multijoint motor behavior", *Exerc. Sport Sci. Rev.*, 15, pp. 153–190, 1987.

C. Hogfors, G. Sigholm and P. Herberts, "Biomechanical model of the human shoulder—I. Elements", *J. Biomech.*, 20, pp. 157–166, 1987.

C. Hogfors, B. Peterson, G. Sigholm and P. Herberts, "Biomechanical model of the human shoulder—II. The shoulder rhythm", *J. Biomech.*, 24, pp. 699–709, 1991.

C. Hogfors, D. Karlsson and B. Peterson, "Structure and internal consistency of a shoulder model", *J. Biomech.*, 28, pp. 767–777, 1995.

K.R.S. Holzbaur, W.M. Murray and S.L. Delp, "A model of the upper extremity for simulating musculoskeletal surgery and analyzing neuromuscular control", *Ann. Biomed. Eng.*, 33(6), pp. 829–840, 2005.

R.E. Hughes and K.N. An, "Monte Carlo simulation of a planar shoulder model", *Med. Biol. Eng. Comput.*, 9, pp. 544–548, 1997.

R.E. Hughes, D.B. Chaffin, S.A. Lavender and G.B.J. Andersson, "Evaluating muscle force prediction models of the lumbar trunk using surface electromyography", *J. Orthop. Res.*, 12, pp. 689–698, 1994.

A. Jinha, R. Ait-Haddou, P. Binding and W. Herzog, "Antagonistic activity of one-joint muscles in three-dimensions using non-linear optimization", *Math. Biosci.*, 202, pp. 57–70, 2006.

D. Karlsson and B. Peterson, "Towards a model for force predictions in the human shoulder", *J. Biomech.*, 25(2), pp. 189–199, 1992.

S. Kumar, "Arm lift strength in work space", *Appl. Ergon.*, 22, pp. 317–328, 1991.

W.A. Latko, T.J. Armstrong, J.A. Foulke and G.D. Herrin, "Development and evaluation of an observational method for assessing repetition in hand tasks", *AIHA*, 58, pp. 278–285, 1997.

B. Laursen, B.R. Jensen, G. Nemeth and G. Sjogaard, "A model predicting individual shoulder muscle forces based on relationship between electromyographic and 3D external forces in static position", *J. Biomech.*, 31, pp. 731–739, 1998.

B. Laursen, B. Sogaard and G. Sjogaard, "Biomechanical model predicting electromyographic activity in three shoulder muscles from 3D kinematics and external forces during cleaning work", *Clin. Biomech.*, 18, pp. 287–295, 2003.

S. Lippitt and F. Matsen, "Mechanisms of glenohumeral joint stability", *Clin. Orthop. Relat. Res.*, 291, pp. 20–28, 1993.

M. Makhsous, "Improvements, validation and adaptation of a shoulder model", Doctoral Dissertation, Chalmers University of Technology, Gothenburg, Sweden, 1999.

L. McAtamney and E.N. Corlett, "RULA: A survey method for the investigation of work-related upper limb disorders", *Appl. Ergon.*, 24(2), pp. 91–99, 1993.

J.S. Moore and A. Garg, "The strain index: a proposed method to analyze jobs for risk of distal upper extremity disorders", *AIHA*, 56(5), pp. 443–458, 1995.

J. Niemi, H. Nieminen, E.P. Takala and E. Viikari-Juntura, "A static shoulder model based on a time-dependent criterion for load sharing between synergistic muscles", *J. Biomech.*, 29, pp. 451–460, 1996.

H. Nieminen, J. Niemi, E.P. Takala and E. Viikari-Juntura, "Load-sharing patterns in the shoulder during isometric flexion tasks", *J. Biomech.*, 28, pp. 555–566, 1995.

B.M. Nigg and W. Herzog, *Biomechanics of the Musculo-skeletal System*, 2nd ed., 1994, pp. 326–329.

M.A. Nussbaum and X. Zhang, "Heuristics for locating upper extremity joint centres from a reduced set of surface markers", *Hum. Mov. Sci.*, 19, pp. 797–816, 2000.

R.J. Shephard, "A personal perspective on aging and productivity with particular reference to physically demanding work", *Ergonomics*, 38, pp. 617–636, 1995.

J.F. Soechting and M. Flanders, "Evaluating an integrated musculoskeletal model of the human arm", *J. Biomech. Eng.*, 119, pp. 93–102, 1997.

G.C. Terry, D. Hammon, P. France and L.A. Norwood, "The stabilizing function of passive shoulder restraints", *Am. J. Sports Med.*, 19, pp. 26–34, 1991.

F.C.T. Van der Helm, "A finite-element musculoskeletal model of the shoulder mechanism", *J. Biomech.*, 5, pp. 551–569, 1994a.

F.C.T. Van der Helm, "Analysis of the kinematic and dynamic behavior of the shoulder mechanism", *J. Biomech.*, 27(5), pp. 527–550, 1994b.

C.L. Vaughan, B.L. Davis and J.C. O'Connor, *Dynamics of Human Gait*, Champaign, IL: Human Kinetics, 1992.

H.E.J. Veeger, F.C.T. Van der Helm, L.H.V. Van der Woude, G.M. Pronk and R.H. Rozendal, "Inertia and musculoskeletal modeling of the shoulder mechanism", *J. Biomech.*, 24(7), pp. 615–629, 1991.

J.E. Wood, S.G. Meek and S.C. Jacobsen, "Quantification of human shoulder anatomy for prosthetic arm control—I. Surface modeling", *J. Biomech.*, 22, pp. 273–292, 1989a.

J.E. Wood, S.G. Meek and S.C. Jacobsen, "Quantification of human shoulder anatomy for prosthetic arm control—II. Anatomy matrices", *J. Biomech.*, 22, pp. 309–325, 1989b.

V. Zatsiorsky and V. Seluyanov, "Estimation of the mass and inertia characteristics of the human body by means of the best predictive regression equations", *Biomechanics IX-B*, Champaign, IL: Human Kinetics, 1993.